Hindawi Publishing Corporation
Journal of Applied Mathematics
Volume 2012, Article ID 421320, 18 pages
doi:10.1155/2012/421320

Research Article

Flow and Heat Transfer of Cu-Water Nanofluid between a Stretching Sheet and a Porous Surface in a Rotating System

M. Sheikholeslami,[1] H. R. Ashorynejad,[2] G. Domairry,[1] and I. Hashim[3,4]

[1] *Department of Mechanical Engineering, Babol University of Technology, Babol, Iran*
[2] *Department of Mechanical Engineering, University of Guilan, Rasht, Iran*
[3] *School of Mathematical Sciences, Universiti Kebangsaan Malaysia, 43600 Bangi, Selangor, Malaysia*
[4] *Solar Energy Research Institute, Universiti Kebangsaan Malaysia, 43600 Bangi, Selangor, Malaysia*

Correspondence should be addressed to I. Hashim, ishak_h@ukm.my

Received 26 January 2012; Revised 15 March 2012; Accepted 15 March 2012

Academic Editor: Srinivasan Natesan

The aim of the present paper is to study the flow of nanofluid and heat transfer characteristics between two horizontal plates in a rotating system. The lower plate is a stretching sheet and the upper one is a solid porous plate. Copper (Cu) as nanoparticle and water as its base fluid have been considered. The governing partial differential equations with the corresponding boundary conditions are reduced to a set of ordinary differential equations with the appropriate boundary conditions using similarity transformation, which is then solved analytically using the homotopy analysis method (HAM). Comparison between HAM and numerical solutions results showed an excellent agreement. The results for the flow and heat transfer characteristics are obtained for various values of the nanoparticle volume fraction, suction/injection parameter, rotation parameter, and Reynolds number. It is shown that the inclusion of a nanoparticle into the base fluid of this problem is capable of causing change in the flow pattern. It is found that for both suction and injection, the heat transfer rate at the surface increases with increasing the nanoparticle volume fraction, Reynolds number, and injection/suction parameter and it decreases with power of rotation parameter.

1. Introduction

The fluid dynamics due to a stretching sheet are important from theoretical as well as practical point of view because of their various applications to polymer technology and metallurgy. During many mechanical forming processes, such as extrusion, melt-spinning, cooling of a large metallic plate in a bath, manufacture of plastic and rubber sheets, glass blowing, continuous casting, and spinning of fibers, the extruded material issues through a

die. Provoked by the process of polymer extrusion in which extradite emerges from a narrow slit, Crane [1] first analyzed the two-dimensional fluid flow over a linearly stretching surface. Later, this problem has been extensively studied in various directions, for example, for non-Newtonian fluids, porous space, and magneto-hydrodynamics [2–5]. It is worth mentioning that, in recent years, interests in flow and heat transfer through porous media have grown considerably, due largely to the demands of such diverse areas such as geophysics, chemical and petroleum industries, building construction, and nuclear reactors [6, 7]. There are very few studies in which authors have considered the channel flow. Borkakoti and Bharali [8] studied the two-dimensional channel flows with heat transfer analysis of a hydromagnetic fluid where the lower plate was a stretching sheet. The flow between two rotating disks has many important technical applications such as in lubrication. Keeping this fact in mind Vajravelu and Kumar [9] studied the effects of rotation on the two-dimensional channel flows. They solved the governing equations analytically and numerically. Fluid heating and cooling are important in many industries fields such as manufacturing and transportation. Effective cooling techniques are absolutely needed for cooling any sort of high-energy device. Common heat transfer fluids such as water, ethylene glycol, and engine oil have limited heat transfer capabilities due to their low heat transfer properties. In contrast, metals thermal conductivities are up to three times higher than the fluids, so it is naturally desirable to combine the two substances to produce a heat transfer medium that behaves like a fluid but has the thermal conductivity of a metal.

Recently, due to the rising demands of modern technology, including chemical production, power station, and microelectronics, there is a need to develop new types of fluids that will be more effective in terms of heat exchange performance. Nanofluids are produced by dispersing the nanometer-scale solid particles into base liquids with low thermal conductivity such as water, ethylene glycol, oils, etc. The term "nanofluid" was first coined by Choi [10] to describe this new class of fluids. The characteristic feature of nanofluids is thermal conductivity enhancement, a phenomenon observed by Masuda et al. [11]. Nanofluids are envisioned to describe fluids in which nanometer-sized particles (usually less than 100 nm in size) are suspended in convectional heat transfer basic fluids. Numerous methods have been taken to improve the thermal conductivity of these fluids by suspending nano/microsized particles in liquids. There have been published several numerical studies on the modeling of natural convection heat transfer in nanofluids recently such as [12–14]. Most scientific problems and phenomena are inherently in form of nonlinearity. Except a limited number of these problems, most of them do not have exact solution. Therefore, these nonlinear equations should be solved using the other methods. Liao [15, 16] proposed a new asymptotic technique for nonlinear ordinary differential equations (ODEs) and partial differential equations (PDEs), named the homotopy analysis method (HAM). Based on the homotopy in topology, the homotopy analysis method contains obvious merits over perturbation techniques: its validity does not depend on small/larger parameters. Thus, the HAM method can be applied to analyze more of the nonlinear problems in science and engineering. Another advantage of the homotopy analysis method is that it provides larger freedom to select initial approximations, auxiliary linear operators, and some other auxiliary parameters. This method does not need small parameters such as the Adomian decomposition method [17] and homotopy perturbation method [18] so it can overcome the restrictions and limitations of perturbation methods. These Analytical methods have already been successfully applied to solve some engineering problems [19–22].

The objective of the present paper is to study the nanofluid flow and heat transfer due to a stretching cylinder with uniform suction/injection. The nanofluid model proposed by

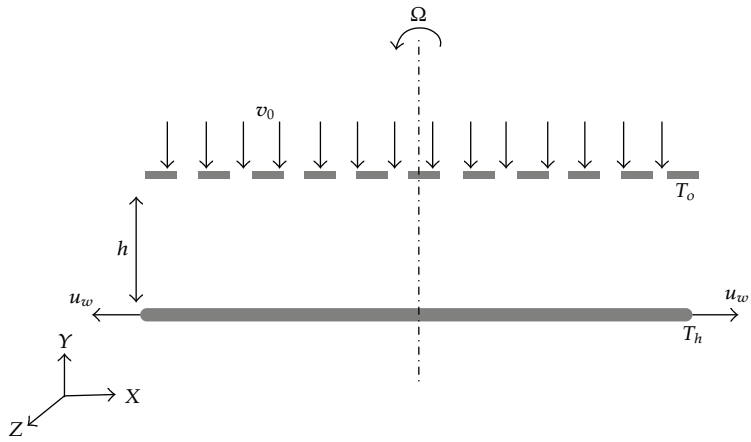

Figure 1: Schematic theme of the problem geometry.

Tiwari and Das [23] is used. Copper (Cu) as nanoparticle and water as its base fluid have been considered. The reduced ordinary differential equations are solved analytically using the homotopy analysis method (HAM). The effects of the parameters governing the problem are studied and discussed.

2. Flow Analysis

2.1. Governing Equations

Consider the steady flow of a nanofluid between two horizontal parallel plates when the fluid and the plates rotate together around the axis, which is normal to the plates with a constant angular velocity of Ω.

A Cartesian coordinate system (x, y, z) is considered as follows: the x-axis is along the plate, the y-axis is perpendicular to it, and the z-axis is normal to the x-y plane (see Figure 1). The origin is located at the lower plate, and the plates are located at $y = 0$ and $y = h$. The lower plate is being stretched by two equal opposite forces so that the position of the point $(0, 0, 0)$ remains unchanged. The upper plate is subjected to a constant wall suction with velocity of v_0 (<0) or a constant wall injection with velocity of v_0 (>0), respectively. The lower and upper plates are maintained at constant hot (T_h) and cold (T_0) temperature, respectively.

The fluid is a water-based nanofluid containing Cu (copper). The nanofluid is a two-component mixture with the following assumptions:

(i) incompressible,

(ii) no-chemical reaction,

(iii) negligible viscous dissipation,

(iv) negligible radiative heat transfer,

(v) nano-solid-particles and the base fluid are in thermal equilibrium and no slip occurs between them.

The thermophysical properties of the nanofluid are given in Table 1 [25].

Table 1: Thermophysical properties of water and nanoparticle [25].

	ρ (kg/m^3)	C_p (j/kgk)	k (W/m·k)	$\beta \times 10^5$ (K^{-1})
Pure water	997.1	4179	0.613	21
Copper (Cu)	8933	385	401	1.67

Under these assumptions and using the nanofluid model proposed by Tiwari and Das [23], the governing equations of motion in a rotating frame of reference are

$$\frac{\partial u}{\partial x} + \frac{\partial v}{\partial y} + \frac{\partial w}{\partial z} = 0, \tag{2.1}$$

$$u\frac{\partial u}{\partial x} + v\frac{\partial u}{\partial y} + 2\Omega w = -\frac{1}{\rho_{\mathrm{nf}}}\frac{\partial p^*}{\partial x} + \upsilon_{\mathrm{nf}}\left(\frac{\partial^2 u}{\partial x^2} + \frac{\partial^2 u}{\partial y^2}\right), \tag{2.2}$$

$$u\frac{\partial v}{\partial y} = -\frac{1}{\rho_{\mathrm{nf}}}\frac{\partial p^*}{\partial y} + \upsilon_{\mathrm{nf}}\left(\frac{\partial^2 v}{\partial x^2} + \frac{\partial^2 v}{\partial y^2}\right), \tag{2.3}$$

$$u\frac{\partial w}{\partial x} + v\frac{\partial w}{\partial y} - 2\Omega w = \upsilon_{\mathrm{nf}}\left(\frac{\partial^2 w}{\partial x^2} + \frac{\partial^2 w}{\partial y^2}\right), \tag{2.4}$$

where u, v, and w denote the fluid velocity components along the x, y, and z directions, p^* is the modified fluid pressure, and the physical meanings of the other quantities are mentioned in the Nomenclature. The absence of $\partial p^*/\partial z$ in (2.4) implies that there is a net cross-flow along the z-axis. The corresponding boundary conditions of (2.1)–(2.4) are

$$\begin{aligned} &u = ax, \quad v = 0, \quad w = 0 \quad \text{at } y = 0, \\ &u = 0, \quad v = v_0, \quad w = 0 \quad \text{at } y = h. \end{aligned} \tag{2.5}$$

The effective density ρ_{nf}, the effective dynamic viscosity μ_{nf}, the effective heat capacity $(\rho C_p)_{\mathrm{nf}}$, and the effective thermal conductivity k_{nf} of the nanofluid are defined as [26]

$$\begin{aligned} \rho_{\mathrm{nf}} &= (1-\phi)\rho_f + \phi\rho_s, \qquad \mu_{\mathrm{nf}} = \frac{\mu_f}{(1-\phi)^{2.5}}, \\ (\rho C_p)_{\mathrm{nf}} &= (1-\phi)(\rho C_p)_f + \phi(\rho C_p)_s, \\ \frac{k_{\mathrm{nf}}}{k_f} &= \frac{k_s + 2k_f - 2\phi(k_f - k_s)}{k_s + 2k_f + 2\phi(k_f - k_s)}, \end{aligned} \tag{2.6}$$

where ϕ is the solid volume fraction of the nanoparticles.

The nondimensional variables are introduced as follows:

$$\eta = \frac{y}{h}, \quad u = axf'(\eta), \quad v = -ahf(\eta), \quad w = axg(\eta), \tag{2.7}$$

where the prime denotes differentiation with respect to η. Substituting (2.7) into (2.2)–(2.4), we obtain

$$-\frac{1}{\rho_{\mathrm{nf}}h}\frac{\partial p^*}{\partial x} = a^2 x\left((f')^2 - ff'' - \frac{f'''}{RA_1(1-\phi)^{2.5}} + \frac{2\mathrm{Kr}}{R}g\right),$$
$$-\frac{1}{\rho_{\mathrm{nf}}h}\frac{\partial p^*}{\partial \eta} = a^2 h\left(ff' + \frac{f''}{RA_1(1-\phi)^{2.5}}\right), \tag{2.8}$$

$$g'' - RA_1(1-\phi)^{2.5}(f'g - fg') + 2\mathrm{Kr}A_1(1-\phi)^{2.5}f' = 0. \tag{2.9}$$

The dimensionless quantities in these equations are the following: A_1 is the nanofluid parameter, R is the Reynolds number, and Kr is the rotation parameter, and they are defined as

$$A_1 = (1-\phi) + \phi\frac{\rho_s}{\rho_f}, \qquad R = \frac{ah^2}{\nu_f}, \qquad \mathrm{Kr} = \frac{\Omega h^2}{\nu_f}. \tag{2.10}$$

Eliminating the pressure gradient terms from (2.8), these equations can be reduced to

$$f''' - RA_1(1-\phi)^{2.5}\left(f'^2 - ff''\right) - 2\mathrm{Kr}A_1(1-\phi)^{2.5}g = A, \tag{2.11}$$

where A is constant. Differentiation of (2.11) with respect to η gives

$$f^{iv} - RA_1(1-\phi)^{2.5}(f'f'' - ff''') - 2\mathrm{Kr}A_1(1-\phi)^{2.5}g' = 0 \tag{2.12}$$

Therefore, the governing momentum equations for this problem are given in the dimensionless form by

$$f^{iv} - RA_1(1-\phi)^{2.5}(f'f'' - ff''') - 2\mathrm{Kr}A_1(1-\phi)^{2.5}g' = 0,$$
$$g'' - RA_1(1-\phi)^{2.5}(f'g - fg') + 2\mathrm{Kr}A_1(1-\phi)^{2.5}f' = 0 \tag{2.13}$$

and are subjected to the boundary conditions

$$f(0) = 0, \quad f'(0) = 0, \quad g(0) = 0,$$
$$f(1) = \lambda, \quad f'(1) = 0, \quad g(1) = 0, \tag{2.14}$$

where $\lambda = v_0/(ah)$ is the dimensionless suction/injection parameter.

The physical quantity of interest in this problem is the skin friction coefficient C_f along the stretching wall, which is defined as

$$C_f = \frac{\tau_w}{\rho_f u_w^2}, \tag{2.15}$$

where τ_w is the shear stress or skin friction along the stretching wall, which is given by

$$\tau_w = \mu_{\mathrm{nf}} \left(\frac{\partial u}{\partial y}\right)_{y=0}. \tag{2.16}$$

Using (2.7), (2.15), and (2.16), we get

$$\widetilde{C}_f = \frac{1}{A_1(1-\phi)^{2.5}}\, f''(0), \tag{2.17}$$

where $\widetilde{C}_f = (Rx/h)C_f$.

2.2. Heat Transfer Analysis

The energy equation of the present problem with viscous dissipation neglected is given by

$$u\frac{\partial T}{\partial x} + v\frac{\partial T}{\partial x} + w\frac{\partial T}{\partial z} = \alpha_{\mathrm{nf}}\left(\frac{\partial^2 T}{\partial x^2} + \frac{\partial^2 T}{\partial y^2} + \frac{\partial^2 T}{\partial z^2}\right), \tag{2.18}$$

where α_{nf} is the thermal diffusivity of the nanofluids and is defined as

$$\alpha_{\mathrm{nf}} = \frac{k_{\mathrm{nf}}}{(\rho C_p)_{\mathrm{nf}}}. \tag{2.19}$$

We look for a solution of (2.18) of the following form:

$$\theta(\eta) = \frac{T - T_0}{T_h - T_0}, \tag{2.20}$$

where T_0 and T_h are temperatures at the lower and upper plates, respectively. Substituting the similarity variables (2.7) and (2.20) into (2.18), we obtain the following ordinary differential equation:

$$\theta'' + \mathrm{Pr}\frac{RA_2}{A_3} f\theta' = 0 \tag{2.21}$$

subject to the boundary conditions

$$\theta(0) = 1, \quad \theta(1) = 0. \tag{2.22}$$

Here, A_2 and A_3 are dimensionless constants given by

$$A_2 = (1-\phi) + \phi\frac{(\rho C_p)_s}{(\rho C_p)_f}, \qquad A_3 = \frac{k_{\mathrm{nf}}}{k_f} = \frac{k_s + 2k_f - 2\phi(k_f - k_s)}{k_s + 2k_f + 2\phi(k_f - k_s)}, \tag{2.23}$$

and $\mathrm{Pr} = \mu_f C_p / k_f$ is the Prandtl number.

The Nusselt number at the lower plate is defined as

$$\mathrm{Nu} = -\frac{hq_w}{k_f(T_0 - T_h)}, \tag{2.24}$$

where q_w is the heat flux from the lower plate and is given by

$$q_w = -k_{\mathrm{nf}}\left(\frac{\partial T}{\partial y}\right)_{y=0}. \tag{2.25}$$

Using (2.24), (2.25), and (2.26), it can be obtained

$$\mathrm{Nu} = -\left(\frac{k_{\mathrm{nf}}}{k_f}\right)\theta'(0), \tag{2.26}$$

3. The HAM Solution of the Problem

According to some previous works like [27], we choose the initial approximate solutions of $f(\eta), g(\eta)$, and $\theta(\eta)$ as follows:

$$\begin{aligned} f_0(\eta) &= (1-2\lambda)\eta^3 + (3\lambda - 2)\eta^2 + \eta, \\ g_0(\eta) &= 0, \\ \theta_0(\eta) &= 1 - \eta, \end{aligned} \tag{3.1}$$

and the auxiliary linear operators are

$$\begin{aligned} L_1(f) &= f^{iv}, \\ L_2(g) &= g'', \\ L_3(\theta) &= \theta''. \end{aligned} \tag{3.2}$$

These auxiliary linear operators satisfy

$$\begin{aligned} &L_1\left(C_0 + C_1\eta + C_2\eta^2 + C_3\eta^3\right), \\ &L_2(C_4 + C_5\eta), \\ &L_3(C_6 + C_7\eta), \end{aligned} \tag{3.3}$$

where C_i $(i = 0,1,2,3,4,5,6,7)$ are constants. Introducing nonzero auxiliary parameters $\hbar_1$, $\hbar_2$, and $\hbar_3$, we develop the zeroth-order deformation problems as follows:

$$(1-p)L[f(\eta;p) - f_0(\eta)] = p\hbar_1 N_1[f(\eta;p), g(\eta;p), \theta(\eta;p)], \tag{3.4}$$

$$f(0;p) = 0, \quad f(1;p) = \lambda, \quad f'(0;p) = 0, \quad f'(1;p) = 1, \tag{3.5}$$

$$(1-p)L[g(\eta;p) - g_0(\eta)] = p\hbar_2 N_2[f(\eta;p), g(\eta;p), \theta(\eta;p)], \tag{3.6}$$

$$g(0;p) = 0, \qquad g(1;p) = 0, \tag{3.7}$$

$$(1-p)L[\theta(\eta;p) - \theta_0(\eta)] = p\hbar_3 N_3[f(\eta;p), g(\eta;p), \theta(\eta;p)], \tag{3.8}$$

$$\theta(0;p) = 1, \qquad \theta(1;p) = 0, \tag{3.9}$$

where nonlinear operators N_1, N_2, and N_3 are defined as

$$\begin{aligned}
&N_1[f(\eta;p), g(\eta;p), \theta(\eta;p)] \\
&= \frac{\partial^4 f(\eta;p)}{\partial\eta^4} - RA_1(1-\phi)^{2.5}\left(\left(\frac{\partial f(\eta;p)}{\partial\eta}\right)\left(\frac{\partial^2 f(\eta;p)}{\partial\eta^2}\right) f(\eta;\ p)\frac{\partial^3 f(\eta;p)}{\partial\eta^2}\right) \\
&\quad - 2KrA_1(1-\phi)^{2.5}\ \frac{\partial g(\eta;p)}{\partial\eta}, \\
&N_2[f(\eta;\ p), g(\eta;\ p), \theta(\eta;\ p)] \\
&= \frac{\partial^2 f(\eta;\ p)}{\partial\eta^2} - RA_1(1-\phi)^{2.5}\left(\left(\frac{\partial f(\eta;p)}{\partial\eta}\right) g(\eta;\ p) - \left(\frac{\partial g(\eta;p)}{\partial\eta}\right) f(\eta;p)\right) \\
&\quad + 2\mathrm{Kr}A_1(1-\phi)^{2.5}\frac{\partial f(\eta;p)}{\partial\eta}, \\
&N_3[f(\eta;p), g(\eta;p), \theta(\eta;p)] \\
&\quad = \frac{\partial^2\theta(\eta;p)}{\partial\eta^2} + \mathrm{Pr}\frac{RA_2}{A_3}\left(\frac{\partial\theta(\eta;p)}{\partial\eta}\right) f(\eta;p).
\end{aligned} \tag{3.10}$$

For $p = 0$ and $p = 1$, we, respectively, have

$$\begin{aligned}
f(\eta;p) &= f_0(\eta), \qquad f(\eta;1) = f(\eta), \\
g(\eta;p) &= g_0(\eta), \qquad g(\eta;1) = g(\eta), \\
\theta(\eta;p) &= \theta_0(\eta), \qquad \theta(\eta;1) = \theta(\eta).
\end{aligned} \tag{3.11}$$

As p increases from 0 to 1, $f(\eta;p)$, $g(\eta;p)$, and $\theta(\eta;p)$ vary, respectively, from $f_0(\eta)$, $g_0(\eta)$, and $\theta_0(\eta)$ to $f(\eta)$, $g(\eta)$, and $\theta(\eta)$. By Taylor's theorem and using (3.11), $f(\eta)$ and $\theta(\eta)$ can be expanded in a power series of p as follows:

$$\begin{aligned}
f(\eta;p) &= f_0(\eta) + \sum_{m=1}^{\infty}(f_m(\eta)p^m),\\
f_m(\tau) &= \frac{1}{m!}\frac{\partial^m f(\eta;p)}{\partial p^m},\\
g(\eta;p) &= g_0(\eta) + \sum_{m=1}^{\infty}(g_m(\eta)p^m),\\
g_m(\tau) &= \frac{1}{m!}\frac{\partial^m g(\eta;p)}{\partial p^m},\\
\theta(\eta;p) &= \theta_0(\eta) + \sum_{m=1}^{\infty}(\theta_m(\eta)p^m),\\
\theta_m(\tau) &= \frac{1}{m!}\frac{\partial^m \theta(\eta;p)}{\partial p^m}.
\end{aligned} \tag{3.12}$$

In which $\hbar_1$, $\hbar_2$, and $\hbar_3$ are chosen in such a way that these series are convergent at $p = 1$. Convergence of the series (3.12) depends on the auxiliary parameters $\hbar_1$, $\hbar_2$, and $\hbar_3$.

Assume that $\hbar_1$ and $\hbar_2$ are selected such that the series (3.12) is convergent at $p = 1$, then due to (3.12) we have

$$\begin{aligned}
f(\eta) &= f_0(\eta) + \sum_{m=1}^{\infty}(f_m(\eta)),\\
g(\eta) &= g_0(\eta) + \sum_{m=1}^{\infty}(g_m(\eta)),\\
\theta(\eta) &= \theta_0(\eta) + \sum_{m=1}^{\infty}(\theta_m(\eta)).
\end{aligned} \tag{3.13}$$

Differentiating the zeroth-order deformation (3.4), (3.6), and (3.8) m times with respect to p and then dividing them by $m!$ and finally setting $p = 0$, we have the following mth-order deformation problem:

$$\begin{aligned}
L_1\left[f_m(\eta) - \chi_m f_{m-1}(\eta)\right] &= \hbar_1 R_m^f(\eta),\\
f(0;p) = 0, \quad f(1;p) = \lambda, \quad f'(0;p) = 0, \quad f'(1;p) &= 1,\\
R_m^f(\eta) \;= f_{m-1}^{IV}&\\
-RA_1(1-\phi)^{2.5}&\left(\left(\sum_{n=0}^{m-1} f_{m-1-n}f_n''\right) - \left(\sum_{n=0}^{m-1} f_{m-1-n}f_n'''\right)\right) - 2\mathrm{Kr}A_1(1-\phi)^{2.5}g_{m-1}',\\
L_2\left[g_m(\eta) - \chi_m g_{m-1}(\eta)\right] &= \hbar_2 R_m^g(\eta),\\
g(0;\,p) = 0, \qquad g(1;\,p) &= 0,
\end{aligned}$$

$$
\begin{aligned}
R_m^g(\eta) \;=\; & g''_{m-1} \\
& -RA_1(1-\phi)^{2.5}\left(\left(\sum_{n=0}^{m-1} g_{m-1-n} f'_n\right) - \left(\sum_{n=0}^{m-1} f_{m-1-n} g'_n\right)\right) + 2\mathrm{Kr}A_1(1-\phi)^{2.5}\; f'_{m-1}, \\
& L_3\left[\theta_m(\eta) - \chi_m \theta_{m-1}(\eta)\right] = \hbar_3 R_m^\theta(\eta), \\
& g(0;\; p) = 0, \qquad g(1;\; p) = 0, \\
& R_m^\theta(\eta) = \; \theta''_{m-1} \; + \; \mathrm{Pr}\frac{RA_2}{A_3}\left(\sum_{n=0}^{m-1} f_{m-1-n}\theta'_n\right).
\end{aligned}
\tag{3.14}
$$

We use MAPLE software to obtain the solution of these equations. We assume $\hbar_1 = \hbar_2 = \hbar_3 = \hbar$, for instance, when $\phi = 0.1$, Kr = 0.5, $R = 0.5$, $\lambda = 0.5$, and Pr = 6.2 (Cu-water). First, deformations of the coupled solutions are presented as follows:

$$
\begin{aligned}
f_1(\eta) &= -0.0009583529265\hbar\eta^6 + 0.00570117560\hbar\eta^5 + 0.0160093065\hbar\eta^4 \\
&\quad - 0.04543500228\hbar\eta^3 + 0.024634207\hbar\eta^2, \\
g_1(\eta) &= 0.690014107\hbar\eta^2 - 0.2300047024\hbar\eta^3 - 0.46000094046\hbar\eta, \\
\theta_1(\eta) &= 0.08477232594\hbar\eta^4 - 0.3390893037\hbar\eta^3 + 0.2543169778\hbar\eta.
\end{aligned}
\tag{3.15}
$$

The solutions $f_2(\eta)$, $g_2(\eta)$ and $\theta_2(\eta)$ were too long to be mentioned here, therefore, they are shown graphically.

4. Convergence of the HAM Solution

As pointed out by Liao [28], the convergence and the rate of approximation for the HAM solution strongly depend on the values of auxiliary parameter $\hbar$. This region of $\hbar$ can be found by plotting $f'''(0)$, $g'(0)$, and $\theta'(0)$ for $\hbar$ ($\hbar$-curve) and choosing $\hbar$, where $f'''(0)$, $g'(0)$, and $\theta'(0)$ are constant. It is worthwhile to be mentioned that for different values of flow parameters $(\phi, \mathrm{Kr}, R, \lambda)$ a new h-curve should be plotted as using a unique $\hbar$-curve for all cases may lead to a considerable error. Therefore, in this study, we have obtained admissible values of $\hbar$ for all cases but only depicted the $\hbar$-curves of $f'''(0)$, $g'(0)$, and $\theta'(0)$ for one case in Figure 2 for brevity.

5. Results and Discussions

The governing equations and their boundary conditions are transformed to ordinary differential equations that are solved analytically using the homotopy analysis method (HAM) and the results compared with numerical method (fourth-order Runge-Kutta) [29]. The results obtained by the homotopy analysis method were well matched with the results carried out by the numerical solution obtained by the four-order Runge-kutta method as shown in Figure 3. In order to test the accuracy of the present results, we have compared the results for the temperature profiles $\theta(\eta)$ with those reported by Mehmood and Ali [24] when $\phi = 0$ (regular or Newtonian fluid) and different values of the Prandtl number.

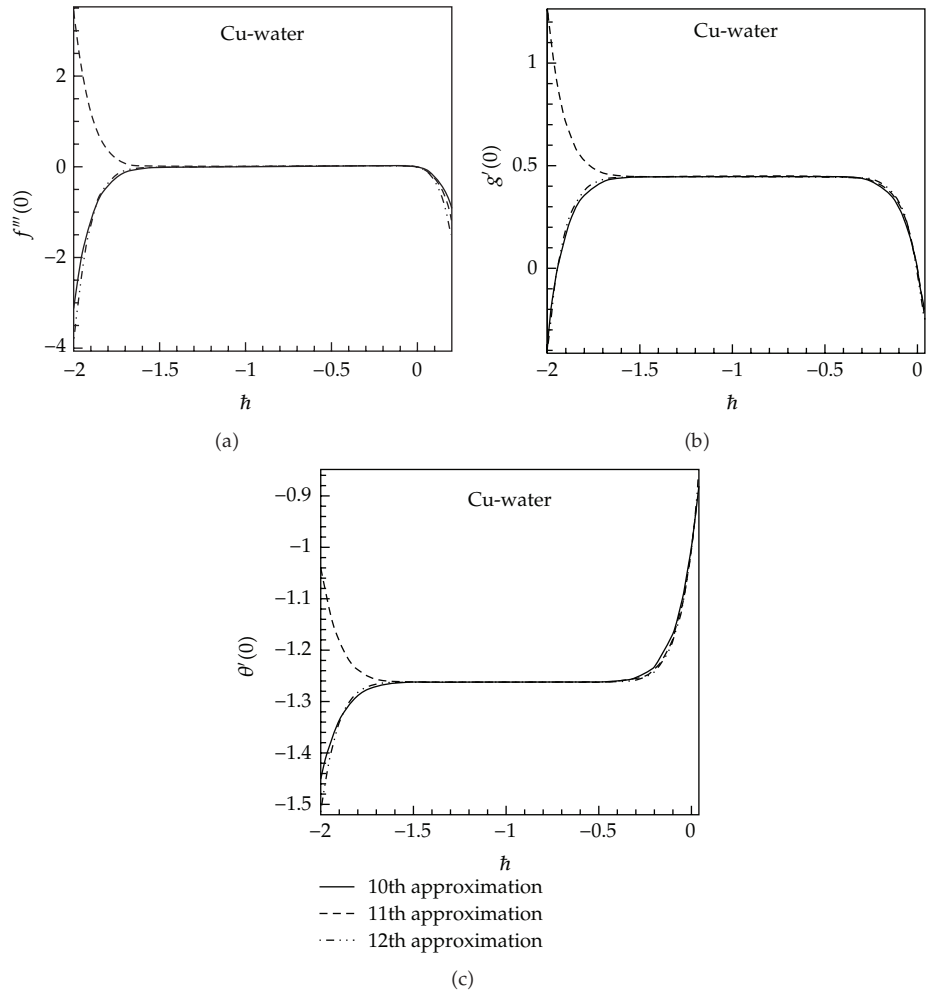

Figure 2: The $\hbar$ curve of (a) $f'''(0)$, (b) $g'(0)$, and (c) $\theta'(0)$ (a) for different orders of approximation when $\phi = 0.1$, Kr = 0.5, $R = 0.5$, $\lambda = 0.5$, and Pr = 6.2, (b) for different values of ϕ when Kr = 0.5, $R = 0.5$, $\lambda = 0.,5$ and Pr = 6.2 at the 12th order of approximation and for different values of λ when Kr = 0.5, $R = 0.5$, and Pr = 6.2 at the 12th order of approximation.

After this validity, results are given for the velocity, temperature distribution, wall shear stress, and Nusselt number for different nondimensional numbers.

Figure 4 shows the effect of nanoparticle volume fraction (ϕ) on (a) velocity profile and (b) temperature distribution when Kr = 0.5, $R = 1$, $\lambda = 0.5$, and Pr = 6.2. Effects of suction/injection parameter (λ) on (a) velocity profile, (b) Temperature distribution, (c) skin friction coefficient, and (d) Nusselt number when Kr = 0.5, $R = 1$, $\phi = 0.1$, and Pr = 6.2 are shown in Figure 5. It has been found that when the volume fraction of the nanoparticle increases from 0 to 0.2, the thickness of the momentum boundary and thermal boundary layer increases (Figure 4). Figures 5(a) and 5(b) show that all boundary layer thicknesses decrease as λ increases from negative (injection) to positive (suction) values. We know that the effect

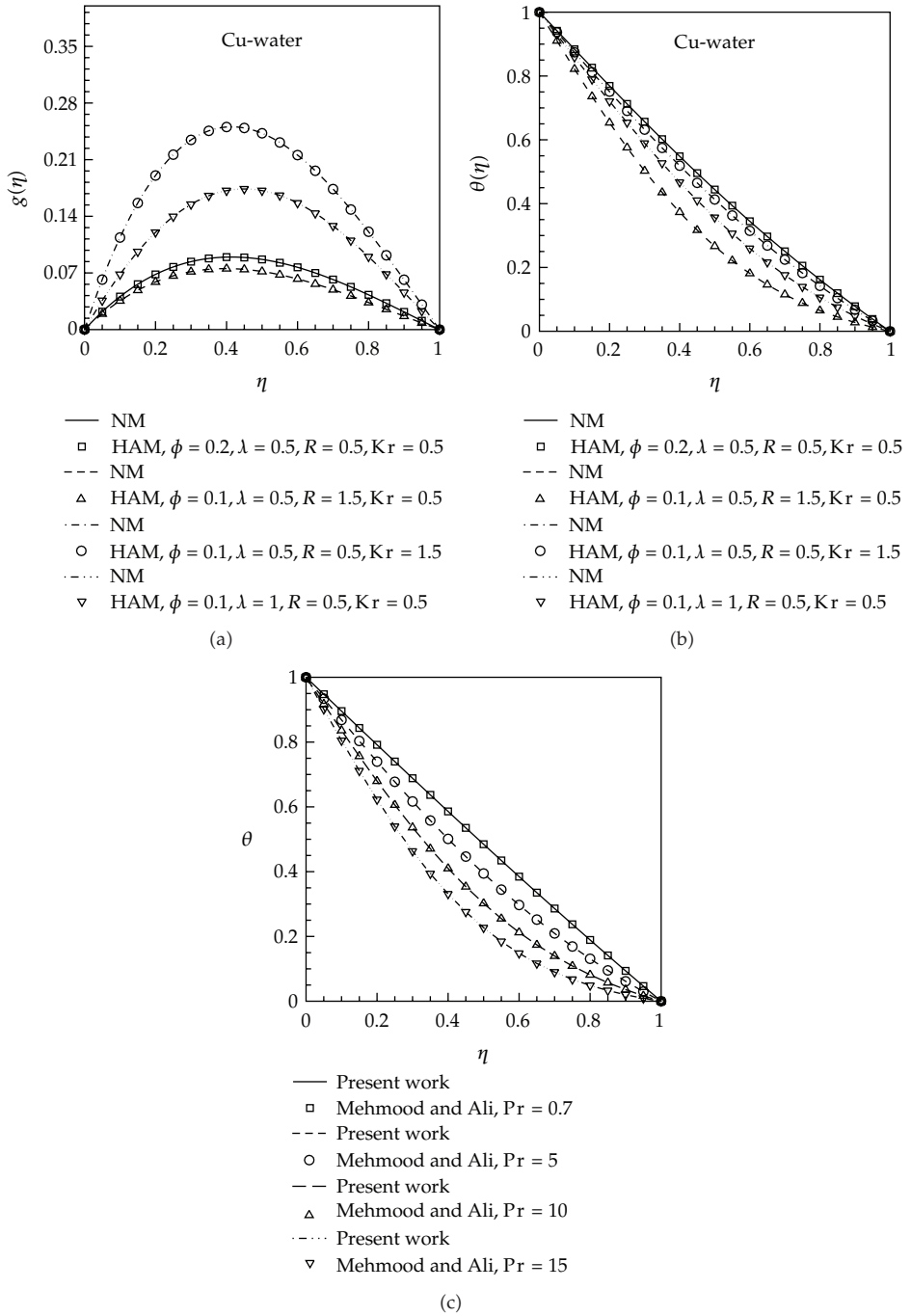

Figure 3: Comparison between numerical results and HAM solution results for (a) $g(\eta)$ and (b) $\theta(\eta)$ when Pr = 6.2; (c) temperature profiles with Mehmood and Ali [24] for $\phi = 0$ (regular fluid), Kr = 0 (nonrotating fluid) when $\varphi = 0$, $\lambda = 0.5$, $M = 1$, $R = 0.5$, and Kr = 0.5.

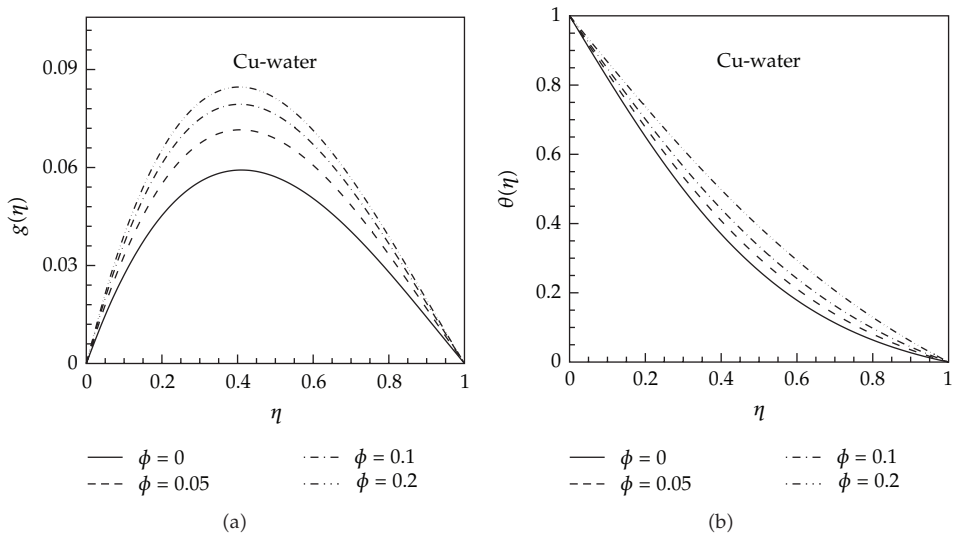

Figure 4: Effect of nanoparticle volume fraction (ϕ) on (a) velocity profile and (b) temperature distribution when Kr = 0.5, $R = 1$, $\lambda = 0.5$, and Pr = 6.2.

of suction is to bring the fluid closer to the surface and, therefore, to reduce the thermal boundary layer thickness, while for injection opposite trend is observed. As suction/injection parameter (λ) increases, the magnetic skin friction coefficient decreases and Nusselt number increases (Figures 5(c) and 5(d)). The sensitivity of thermal boundary layer thickness to volume fraction of nanoparticles is related to the increased thermal conductivity of the nanofluid. In fact, higher values of thermal conductivity are accompanied by higher values of thermal diffusivity. The high value of thermal diffusivity causes a drop in the temperature gradients and accordingly increases the boundary thickness as demonstrated in Figure 4(b). This increase in thermal boundary layer thickness reduces the Nusselt number; however, according to (2.26), the Nusselt number is a multiplication of temperature gradient and the thermal conductivity ratio (conductivity of the of the nanofluid to the conductivity of the base fluid). Since the reduction in temperature gradient due to the presence of nanoparticles is much smaller than thermal conductivity ratio, an enhancement in Nusselt takes place by increasing the volume fraction of nanoparticles as it can be seen in Figures 5(c) and 5(d). Also Figure 5(c) indicates that increasing nanoparticle volume fraction leads to decrease in magnitude of the skin friction coefficient.

Figure 6 displays the effects of Reynolds number (R) on (a) velocity profile, (b) temperature distribution, (c) skin friction coefficient, and (d) Nusselt number when Kr = 0.5, $\lambda = 0.5$, $\phi = 0.1$, and Pr = 6.2. It is worth to mention that the Reynolds number indicates the relative significance of the inertia effect compared to the viscous effect. Thus, both velocity and temperature profiles decrease as Re increase and in turn increasing Reynolds number leads to increase in the magnitude of the skin friction coefficient and Nusselt number (Figure 6).

Figure 7 shows the effects of rotation parameter (Kr) on (a) velocity profile, (b) temperature distribution (c) skin friction coefficient, and (d) Nusselt number when $R = 1$, $\lambda = 0.5$, $\phi = 0.1$, and Pr = 6.2. Increasing rotation parameter leads to Coriolis force increase that causes both velocity and temperature profiles to increase. Also increasing

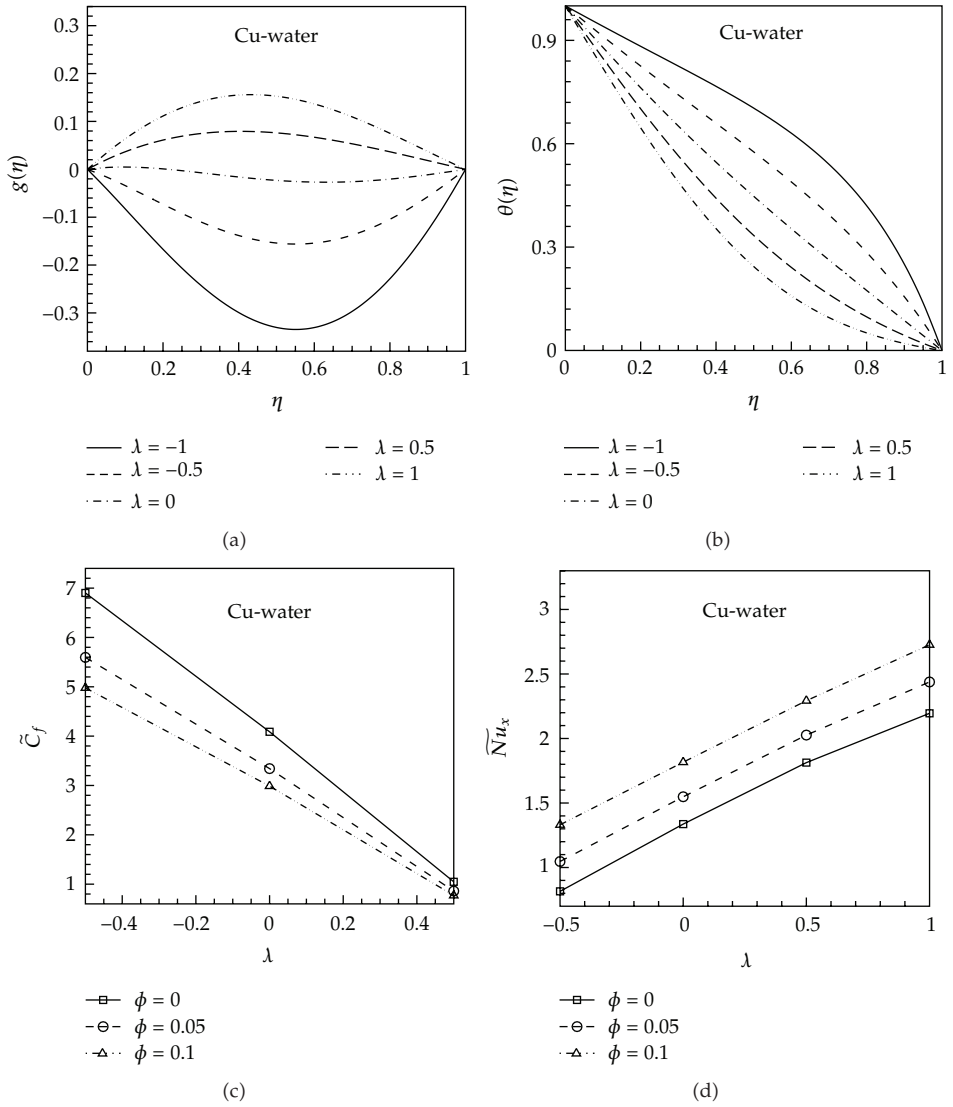

Figure 5: Effect of suction/injection parameter (λ) on (a) velocity profile, (b)temperature distribution, (c) skin friction coefficient, and (d) Nusselt number when Kr = 0.5, $R = 1$, $\phi = 0.1$, and Pr = 6.2.

rotation parameter leads to decreasing the magnitude of the skin friction coefficient and Nusselt number.

6. Conclusions

In the present paper the three-dimensional nanofluid flow between two horizontal parallel plates in which plates rotate together is considered. The problem is solved analytically using the homotopy analysis method (HAM). The results compared with numerical method (fourth-order Runge-Kutta) results. Effects of nanoparticle volume fraction, suction/injection parameter, Reynolds number, and rotation parameter on the flow and heat transfer

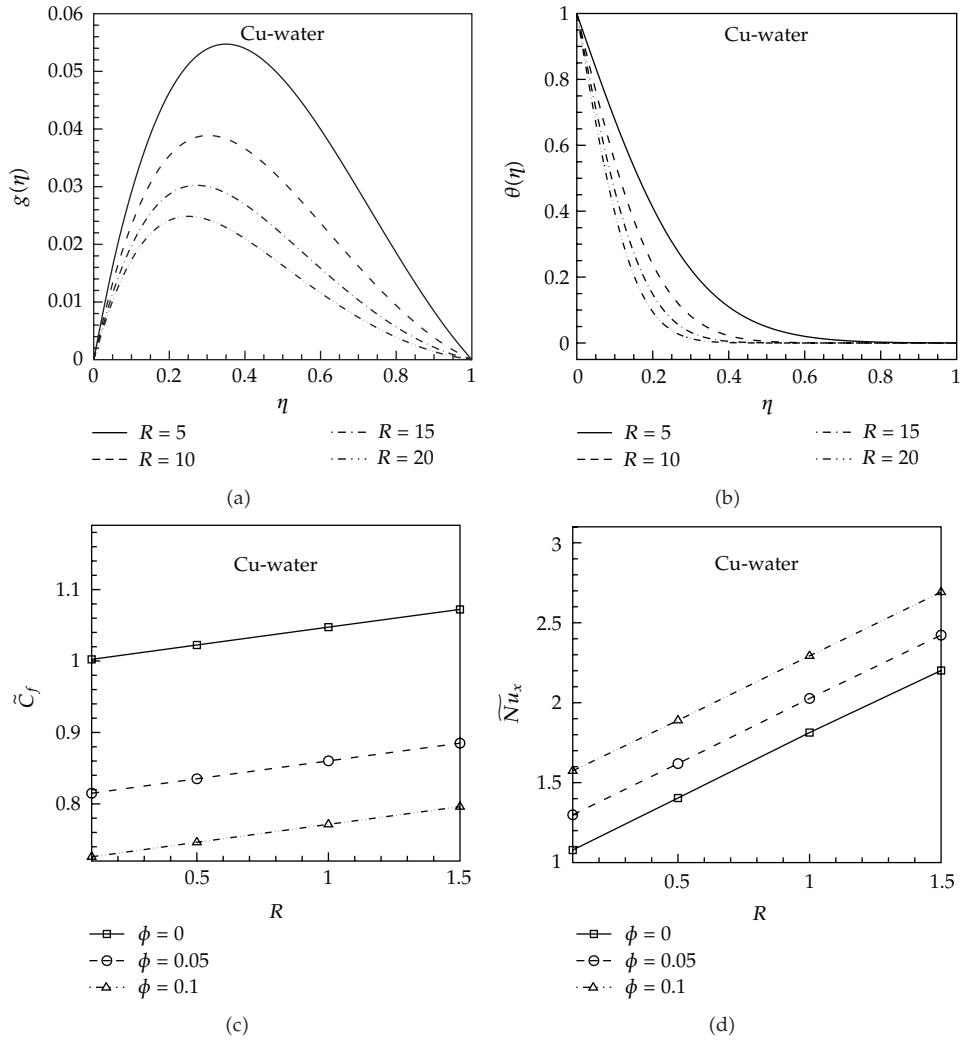

Figure 6: Effect of Reynolds number (R) on (a) velocity profile, (b) temperature distribution, (c) skin friction coefficient, and (d) Nusselt number when Kr = 0.5, $\lambda = 0.5$, $\phi = 0.1$, and Pr = 6.2.

characteristics have been examined. Some conclusions obtained from this investigation are summarized as follows.

(a) The magnitude of the skin friction coefficient increases as the rotation parameter increases, but it decreases as each of nanoparticle volume fraction, Reynolds number, and injection/suction parameter increases.

(b) Nusselt number has direct relationship with nanoparticle volume fraction, Reynolds number, and injection/suction parameter, while it has reverse relationship with power of rotation parameter.

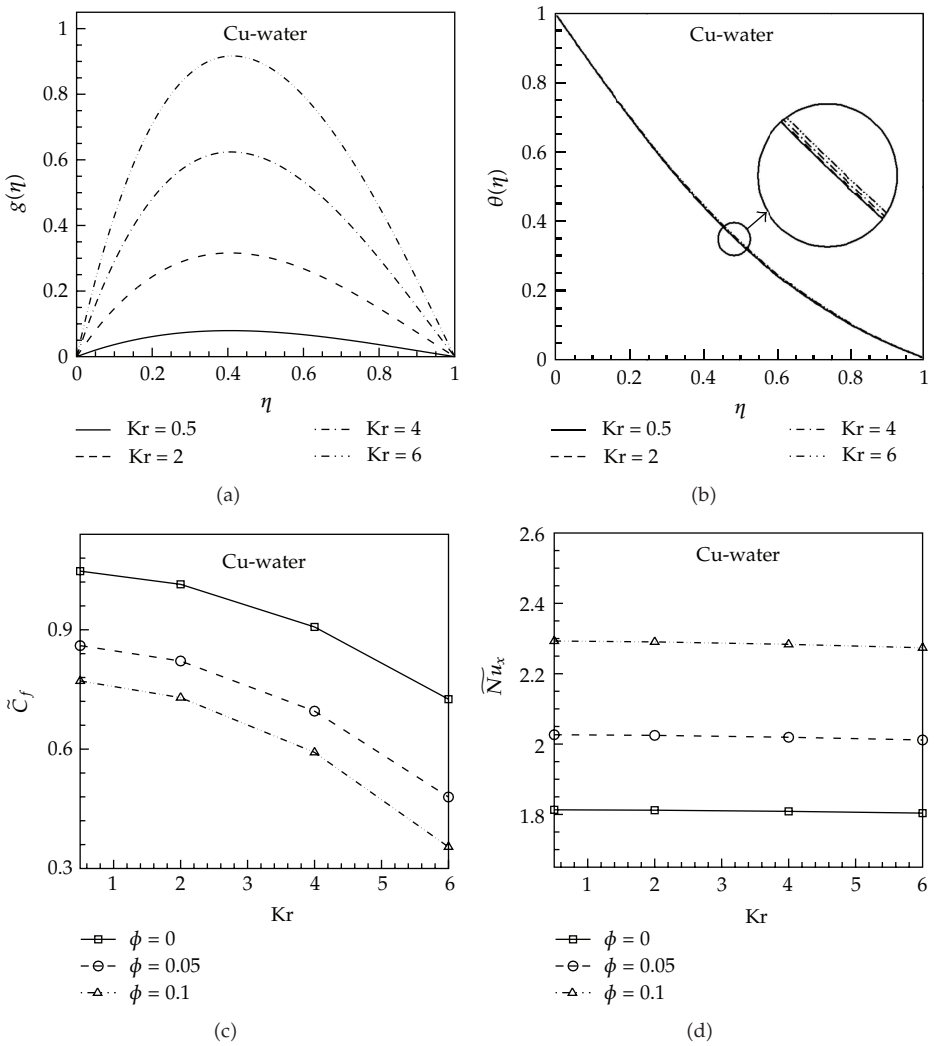

Figure 7: Effect of rotation parameter (Kr) on (a) velocity profile, (b) temperature distribution, (c) skin friction coefficient, and (d) Nusselt number when $R = 1$, $\lambda = 0.5$, $\phi = 0.1$, and Pr = 6.2.

Nomenclature

A_1, A_2, A_3:	Dimensionless constants
C_p:	Specific heat at constant pressure
$C_f, \widetilde{C}_f$:	Skin friction coefficients
$f(\eta)$, $g(\eta)$:	Similarity functions
L_1, L_2, L_3:	Auxiliary linear operators
$\hbar$:	Nonzero auxiliary parameter
h:	Distance between the plates
k:	Thermal conductivity
Kr:	Rotation parameter
N_1, N_2, N_3:	Nonlinear operators

Nu: Nusselt number
p^*: Modified fluid pressure
Pr: Prandtl number
q_w: Heat flux at the lower plate
R: Reynolds number
u, v, w: Velocity components along x, y, and z axes, respectively
$u_w(x)$: Velocity of the stretching surface
v_0: Suction/injection velocity.

Greek Symbols

α: Thermal diffusivity
η: Dimensionless variable
θ: Dimensionless temperature
ρ: Density
ϕ: Nanoparticle volume fraction
λ: Dimensionless suction/injection parameter
μ: Dynamic viscosity
υ: Kinematic viscosity
σ: Electrical conductivity
τ_w: Skin friction or shear stress along the stretching surface
Ω: Constant rotation velocity.

Subscripts

∞: Condition at infinity
nf: Nanofluid
f: Base fluid
s: Nano-solid-particles.

References

[1] L. J. Crane, "Flow past a stretching plate," *Zeitschrift für angewandte Mathematik und Physik ZAMP*, vol. 21, no. 4, pp. 645–647, 1970.
[2] P. S. Gupta and A. S. Gupta, "Heat and mass transfer on a stretching sheet with suction or blowing," *The Canadian Journal of Chemical Engineering*, vol. 55, pp. 744–746, 1977.
[3] C. K. Chen and M. I. Char, "Heat transfer of a continuous, stretching surface with suction or blowing," *Journal of Mathematical Analysis and Applications*, vol. 135, no. 2, pp. 568–580, 1988.
[4] A. Ishak, R. Nazar, and I. Pop, "Boundary layer flow and heat transfer over an unsteady stretching vertical surface," *Meccanica*, vol. 44, no. 4, pp. 369–375, 2009.
[5] B. McLeod and K. R. Rajagopal, "On the non-uniqueness of the flowof a NaviereStokes fluid due to stretching boundary," *Archive for Rational Mechanics and Analysis*, vol. 98, pp. 385–493, 1987.
[6] P. Vadasz, Ed., *Emerging Topics in Heat and Mass Transfer in Porous Media*, Springer, New York, NY, USA, 2008.
[7] K. Vafai, Ed., *Handbook of Porous Media*, Taylor & Francis, New York, NY, USA, 2nd edition, 2005.

[8] A. K. Borkakoti and A. Bharali, "Hydromagnetic flow and heat transfer between two horizontal plates, the lower plate being a stretching sheet," *Quarterly of Applied Mathematics*, vol. 40, no. 4, pp. 461–467, 1982/83.
[9] K. Vajravelu and B. V. R. Kumar, "Analytical and numerical solutions of a coupled non-linear system arising in a three-dimensional rotating flow," *International Journal of Non-Linear Mechanics*, vol. 39, no. 1, pp. 13–24, 2004.
[10] S. Choi, "Enhancing Thermal Conductivity of Fluids With Nanoparticles in Developments and Applications of Non-Newtonian Flows," *ASME*, vol. 66, pp. 99–105, 1995.
[11] H. Masuda, A. Ebata, K. Teramae, and N. Hishinuma, "Alteration of thermal conductivity and viscosity of liquid by dispersing ultra-fine particles," *Netsu Bussei*, vol. 7, pp. 227–233, 1993.
[12] D. Domairry, M. Sheikholeslami, H. R. Ashorynejad, R. S. R. Gorla, and M. Khani, "Natural convection flow of a non-Newtonian nanofluid between two vertical flat plates," *Proceedings of the Institution of Mechanical Engineers, Part N: Journal of Nanoengineering and Nanosystems*, vol. 225, no. 3, pp. 115–122, 2012.
[13] R. S. R. Gorla and A. Chamkha, "Natural convective boundary layer flow over a horizontal plate embedded in a porous medium saturated with a nanofluid," *Journal of Modern Physics*, vol. 2, pp. 62–71, 2011.
[14] S. Soleimani, M. Sheikholeslami, D. D. Ganji, and M. Gorji-Bandpay, "Natural convection heat transfer in a nanofluid filled semi-annulus enclosure," *International Communications in Heat and Mass Transfer*, vol. 39, no. 4, pp. 565–574, 2012.
[15] S.-J. Liao, "An explicit, totally analytic approximate solution for Blasius' viscous flow problems," *International Journal of Non-Linear Mechanics*, vol. 34, no. 4, pp. 759–778, 1999.
[16] S.-J. Liao, "A uniformly valid analytic solution of two-dimensional viscous flow over a semi-infinite flat plate," *Journal of Fluid Mechanics*, vol. 385, pp. 101–128, 1999.
[17] M. Sheikholeslami, D. D. Ganji, H. R. Ashorynejad, and H. B. Rokni, "Analytical investigation of Jeffery-Hamel flow with high magnetic field and nano particle by Adomian decomposition method," *Applied Mathematics and Mechanics (English Edition)*, vol. 33, no. 1, pp. 1553–1564, 2012.
[18] M. Sheikholeslami, H. R. Ashorynejad, D. D. Ganji, and A. Kolahdooz, "Investigation of rotating MHD viscous flow and heat transfer between stretching and porous surfaces using analytical method," *Mathematical Problems in Engineering*, vol. 2011, Article ID 258734, 17 pages, 2011.
[19] M. Hassani, M. Mohammad Tabar, H. Nemati, G. Domairry, and F. Noori, "An analytical solution for boundary layer flow of a nanofluid past a stretching sheet," *International Journal of Thermal Sciences*, vol. 50, no. 11, pp. 2256–2263, 2011.
[20] M. Esmaeilpour, G. Domairry, N. Sadoughi, and A. G. Davodi, "Homotopy analysis method for the heat transfer of a non-Newtonian fluid flow in an axisymmetric channel with a porous wall," *Communications in Nonlinear Science and Numerical Simulation*, vol. 15, no. 9, pp. 2424–2430, 2010.
[21] M. Sheikholeslami, H. R. Ashorynejad, D. D. Ganji, and A. Yıldırım, "Homotopy perturbation method for three-dimensional problem of condensation film on inclined rotating disk," *Scientia Iranica*. In press.
[22] G. Domairry and N. Nadim, "Assessment of homotopy analysis method and homotopy perturbation method in non-linear heat transfer equation," *International Communications in Heat and Mass Transfer*, vol. 35, no. 1, pp. 93–102, 2008.
[23] R. K. Tiwari and M. K. Das, "Heat transfer augmentation in a two-sided lid-driven differentially heated square cavity utilizing nanofluids," *International Journal of Heat and Mass Transfer*, vol. 50, no. 9-10, pp. 2002–2018, 2007.
[24] A. Mehmood and A. Ali, "Analytic solution of three-dimensional viscous flow and heat transfer over a stretching flat surface by homotopy analysis method," *Journal of Heat Transfer*, vol. 130, no. 12, pp. 21701-1–21701-7, 2008.
[25] H. F. Oztop and E. Abu-Nada, "Numerical study of natural convection in partially heated rectangular enclosures filled with nanofluids," *International Journal of Heat and Fluid Flow*, vol. 29, no. 5, pp. 1326–1336, 2008.
[26] M. Kaviany, *Principles of Heat Transfer in Porous Media*, Springer, New York, NY, USA, 1992.
[27] N. Nadim and G. Domairry, "Analytical study of natural convection in high Prandtl number," *Energy Conversion and Management*, vol. 50, no. 4, pp. 1056–1061, 2009.
[28] S. Liao, *Beyond Perturbation: Introduction to the Homotopy Analysis Method*, vol. 2 of *CRC Series: Modern Mechanics and Mathematics*, Chapman & Hall/CRC, Boca Raton, Fla, USA, 2004.
[29] E. Fehlberg, "Low-order classical Runge–Kutta formulas with step size control," NASA TR R-315, 1982.